OPTICAL ISSUES FOR THE DIAGNOSTIC STATIONS FOR THE ELI-NP COMPTON GAMMA SOURCE

M. Marongiu*[1], A. Mostacci[1], L. Palumbo[1], Sapienza University, Rome, Italy
E. Chiadroni, F. Cioeta, G. Di Pirro, G. Franzini, V.Shpakov, A. Stella, A. Variola,
LNF-INFN, Frascati, Italy
L. Sabato, University of Sannio, Benevento, Italy
D. Cortis, INFN, Rome, Italy
A. Cianchi, Università di Roma II Tor Vergata, Rome, Italy
[1]also at INFN, Rome, Italy

Abstract

A high brightness electron Linac is being built in the Compton Gamma Source at the ELI Nuclear Physics facility in Romania. To achieve the design luminosity, a train of 32 bunches, 16 ns spaced, with a nominal charge of 250 pC will collide with the laser beam in the interaction point. Electron beam spot size is measured with optical transition radiation (OTR) profile monitors. In order to measure the beam properties, the optical radiation detecting system must have the necessary accuracy and resolution. This paper deals with the studies of different optic configurations to achieve the magnification, resolution and accuracy in order to measure very small beam (below 30 µm) or to study the angular distribution of the OTR and therefore the energy of the beam. Several configurations of the optical detection line will be studied both with simulation tools (e.g. Zemax) and experimentally. The paper will deal also with the sensibility of optic system (in terms of depth of field, magnification and resolution) to systematic errors.

INTRODUCTION

The Gamma Beam Source [1] (GBS) machine is an advanced source of up to ≈20 MeV Gamma Rays based on Compton back-scattering, i.e. collision of an intense high power laser beam and a high brightness electron beam with maximum kinetic energy of about 740 MeV. The Linac will provide trains of bunches in each RF pulse, spaced by the same time interval needed to recirculate the laser pulse in a properly conceived and designed laser recirculator, in such a way that the same laser pulse will collide with all the electron bunches in the RF pulse, before being dumped. The final optimization foresees trains of 32 electron bunches separated by 16 ns, distributed along a 0.5 µs RF pulse, with a repetition rate of 100 Hz.

The goal of this paper is the characterization of different lenses in terms of resolution and magnification for the optical diagnostics for the ELI-NP-GBS LINAC. The optical diagnostics systems in ELI-NP-GBS will provide an interceptive method to measure beam spot size in different positions along the LINAC.

In a typical monitor setup, the beam is imaged via OTR or YAG screen using standard lens optics, and the recorded intensity profile is a measure of the particle beam spot [2]. In conjunction with other accelerator components, it will also be possible to perform various measurements on the beam, namely: its energy and energy spread (with a dipole or corrector magnet), bunch length [3] (with a RF deflector), Twiss parameters [4] (by means of quadrupole scan) or in general 6D characterization on bunch phase space [5]. Such technique is common in conventional [6] and unconventional [7, 8] high brightness LINACs.

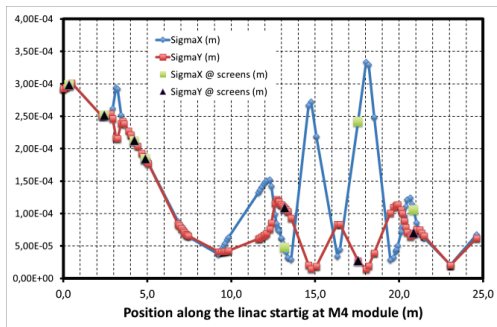

Figure 1: Spot size of the beam in the low energy line after S-band photoinjector.

The expected beam rms size along the LINAC, provided by preliminary beam dynamics simulation, will vary in the 30 µm - 1000 µm range [9] (as reported in Figure 1). An evaluation has been done in order to find the best lenses setups that fit the requirements in term of resolution and magnification for each diagnostic station. The optical acquisition system is constituted by the CCD camera "Basler scout A640-70gm" with a macro lens (see Figure 2). A movable slide is used to place the lens plus camera system closer or farer from the OTR target; such distance is between 60 cm and 130 cm from the OTR target due to mechanical and geometric constraints. In order to avoid possible damage of the optics devices due to the radiation emitted by the beam, a 45° mirror is placed at 40 cm from the target leading to a minimum distance achievable of 60 cm; since the beam pipe is placed 1.5 m from the floor, the maximum distance is instead 130 cm.

The magnification and the resolution of the images for various lens setup have been measured using a "Thorlabs" Calibration target based on the well known "USAF 1951" target.

* marco.marongiu@uniroma1.it

Figure 2: The ELI-GBS optic setup with a camera "Basler Scout A640-70gm" and a macro lens mounted in a movable slide.

MAGNIFICATION

In order to estimate the magnification (M) one need to count the number of pixels (N) of a known size object (L): knowing the pixel size of the camera sensor (R), it will be $M = RN/L$. On the top border of each silicon OTR target a series of lines made of aluminum has been deposited for calibration purpose; the measurements presented in this paper, instead, refer to an "USAF" calibration target that allows also resolution evaluations. The measurements with the OTR, as expected, do not differ from the presented ones. The "USAF" target is characterized by different series of black lines with a millimeter length equal to $2.5/x$, and a millimeter width of $0.5/x$; here the parameter x depends on which series of lines one decides to analyze. This parameter can be calculated with the formula $x = 2^{Group+(Element-1)/6}$, where *Group* and *Element* define the series of line chosen [10]. The results are summerized in the Figure 3; it can be seen that the only lens that allows to reach a magnification equal to 1 is the 180 mm with a teleconverter 2x. On the other hand, the increase of the focal length (f) limits the minimum magnification achievable in the same distance range; hence, a compromise between maximum magnification and a higher flexibility in magnification values needs to be done.

Lenses with higher focal length (i.e. 300 mm) can not be used with the current diagnostic stations due to dimension issues. The field of view is a parameter strictly related to the magnification; it depends on the camera sensor size and the pixel size. Therefore, the horizontal field of view is given by $W_{[px]}R/M$ with W the sensor width expressed in pixels; for the vertical one, one must substitute the width with the hight. In the case of the camera used, this dimension are 659 px and 494 px respectively; therefore, since the pixel size is 7.4 µm, the minimum field of view observed thus far is approximatively 5 mm x 4 mm. Taking in consideration the expected misalignment in the GBS machine, this field of view is big enough to allow the imaging of an off center beam.

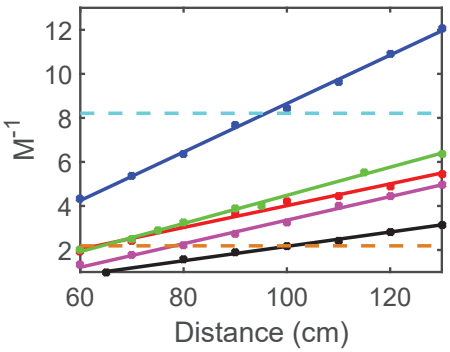

Figure 3: Inverse of the magnification as a function of the distance between the target and the camera sensor for different objective. The blue line (fit) and dot (data) represent the 105 mm; the red ones the 105 mm with teleconverter 2x; the green ones the 180 mm; the black ones the 180 mm with teleconverter 2x and the magenta ones the 180 mm with teleconverter 1.4x. The dashed cyan line represents the magnification required in order to image all the OTR target (3 cm), while the brown one represents the magnification needed for imaging a beam of 1 mm size (see Table 1).

DEPTH OF FIELD

Since in most of the LINAC the diagnostics is based on target with a tilted angle (typically 45°), one needs to take into account also the depth of field [11]; it represents the maximum distance from the focusing plane beyond which the object is not focused anymore. There is a front depth of field (Δx_F) that concerns objects closer to the CCD camera sensor, and a rear one (Δx_R) that concerns objects farer from it. Analytically, they can be expressed as in Eq. 1, 2; f represents the focal length, R is the pixel size, while $\varnothing$ is the effective diameter of the lens, taking therefore into account the diaphragm aperture.

$$\Delta x_R = \frac{(M+1)f}{M(\frac{M^2\varnothing}{R} - 1)} \quad (1)$$

$$\Delta x_F = \frac{(M+1)f}{M(\frac{M^2\varnothing}{R} + 1)} \quad (2)$$

It can be seen from the equations and from Figure 4 that a closer diaphragm increase the depth of field.

RESOLUTION

In order to evaluate the resolution, the "USAF" target has been used. One need to find the smaller line series which are still distinguishable; they are considered so if the contrast function is greater or equal to 0.1. The contrast function is defined as the ratio between the difference and the sum of

ISBN 978-3-95450-182-3

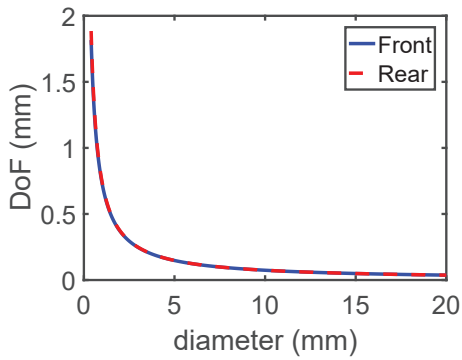

Figure 4: Depth of field front (blue line) and rear (red line) as a function of the effective diameter of the lens for a 50 mm objective, magnification equal to 1 and a pixel size of 7.4 µm.

the intensity values of a black line and the following white space.

Another method to evaluate the resolution is based on the analysis of Modulation Transfer Function (MTF): the MTF is the Fourier transform of the Line Spread Function (LSF) which is the derivative of the edge profile of the black rectangle of the "USAF" target [12]. The abscissa at which the MTF is equal to 0.1 represents the maximum line pairs per millimeters achievable; of course, the inverse of it is the resolution.

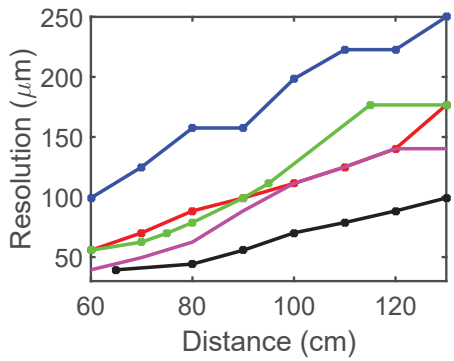

Figure 5: Resolution as a function of the distance between the target and the camera sensor for different lens applying the contrast function method. The blue line (fit) and dot (data) represent the 105 mm; the red ones the 105 mm with teleconverter 2x; the green ones the 180 mm; the black ones the 180 mm with teleconverter 2x and the magenta ones the 180 mm with teleconverter 1.4x.

The measurements showed in Figure 5 are taken using the first method; they show that the 180 mm lens with teleconverter 2x is the best choice, with a resolution of 31 µm.

In order to obtain a good flexibility (in terms of magnification), lenses with variable focal length (in the 75 mm - 200 mm range) were tested also: however, the results in terms of resolution did not meet the requirements.

A camera with a different pixel size (3.75 µm) has been tested too; however, the overall resolution does not change too much (≈ 13%). This is because the contribution of camera sensor to the overall resolution is small with respect to the other contribution related to the objective, lens aberrations, etc.

The resolution determines how accurate can be a measurement of the beam spot size; a finite resolution imply an uncertainty on the position of each pixel of the acquired beam image. Therefore, one can imagine a "macro-pixel" with dimension equal to the resolution: hence, the effect of a finite resolution is a down sample of the beam distribution with potentially negative effect on the evaluation of the position and size of the beam. Assuming a Gaussian transverse

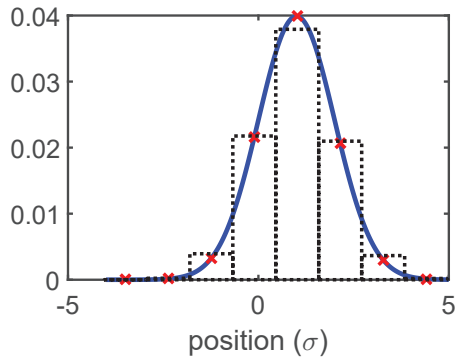

Figure 6: Gaussian distribution considered in $\pm 4\sigma$ down sampled with 8 samples (red asterisk); the black rectangles represents the area where the integral has been calculated.

profile for the beam, one can consider the full beam included in $\pm 4\sigma$. Due to the down sampling, the Gaussian curve is characterized by a number of points (samples) related to the resolution, and their intensities are given by the integral of the black rectangles as seen in Figure 6. These values do not coincide with the exact value of the Gaussian curve and they get closer to them with the increase of the number of samples, hence with a better resolution. One can estimate the mean and the standard deviation from this samples and, comparing them with that of the original distribution, one gets an evaluation of the accuracy. In Figure 7 these results are summarized: it can be seen that the error in the accuracy decays quite rapidly, and it became negligible with about 20 samples for the evaluation of the σ and 10 samples for the mean. Indeed, the mean value of the Gaussian distribution is less affected.

It is interesting to note that an error below 4 % is achieved with 8 samples in $\pm 4\sigma$, hence the resolution is equal to the σ value. Therefore, with a resolution of 30 µm, it is possible to measure with acceptable accuracy beams with σ not smaller than 30 µm; or else, in order to measure accurate enough a beam with a 10 µm σ, one need to achieve at least a resolution of 10 µm.

CONCLUSION

As it has been shown , the diagnostic station geometry combined with the requirements of the GBS machine limit

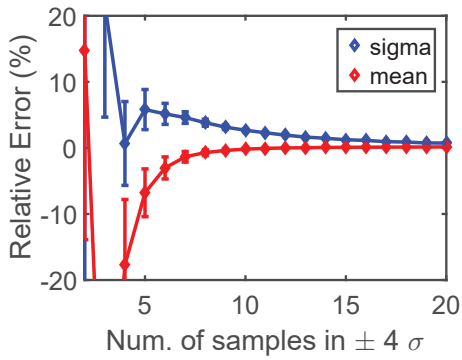

Figure 7: Accuracy relative error of the mean (red) and the σ (blue) (and relative error bars) of a Gaussian distribution as a function of the number of samples achieved in $\pm 4\sigma$ (averaged over 300 measurements).

the possibility of a flexible optic design and the possibility to replicate the same station in all the locations. In Table 1 the choice made thus far are presented; due to specific requirements, in some stations a completely different design may be used (i.e. the study of a setup for energy measurements by means of OTR is ongoing).

Table 1: Optical System proposed for ELI-NP-GBS in order to measure the spot size of the beam (all the lenses are equipped with a teleconverter 2x). The positions are referred as distance from the cathode; in bold character is shown the interaction point.

Positions (m)	Beam size (µm)	Lens (mm)
1.4	1000	105
5	500	105
9	400	105
11	280	105
13	250	105
15	180	180
14	220	180
22	100	105
26	80	180
30	**27**	**180**
36	65	180
37	100	105

Furthermore, some accuracy measurement issues may exist with very small beams (i.e. during the emittance measurement with the quadrupole scan, the weist is expected to be around 10 µm [9]).

Finally, more studies need to be done in order to limit as much as possible defocusing effects: it is well known that they affects the overall resolution [13]; furthermore, it has been shown in recent study, the possibility to take advantage from a dedicated defocused optical system in order to resolve very small beam [14].

REFERENCES

[1] A. Bacci *et al.*, "Electron linac design to drive bright Compton back-scattering gamma-ray sources," *Journal of Applied Physics*, vol. 113, no. 19, p. 194508, 2013.

[2] M. Marongiu *et al.*, "Thermal behavior of the optical transition radiation screens for the eli-np compton gamma source," *Nuclear Instruments and Methods in Physics Research Section A: Accelerators, Spectrometers, Detectors and Associated Equipment*, 2016. [Online]. Available: 10.1016/j.nima.2016.07.040

[3] D. Filippetto *et al.*, "Phase space analysis of velocity bunched beams," *Physical Review Special Topics-Accelerators and Beams*, vol. 14, no. 9, p. 092804, 2011.

[4] A. Mostacci *et al.*, "Chromatic effects in quadrupole scan emittance measurements," *Physical Review Special Topics-Accelerators and Beams*, vol. 15, no. 8, p. 082802, 2012.

[5] A. Cianchi *et al.*, "Six-dimensional measurements of trains of high brightness electron bunches," *Physical Review Special Topics-Accelerators and Beams*, vol. 18, no. 8, p. 082804, 2015.

[6] D. Alesini *et al.*, "Status of the sparc project," *Nuclear Instruments and Methods in Physics Research Section A: Accelerators, Spectrometers, Detectors and Associated Equipment*, vol. 528, no. 1, pp. 586–590, 2004.

[7] P. Antici *et al.*, "Laser-driven electron beamlines generated by coupling laser-plasma sources with conventional transport systems," *Journal of Applied Physics*, vol. 112, no. 4, p. 044902, 2012.

[8] A. R. Rossi *et al.*, "The external-injection experiment at the sparc_lab facility," *Nuclear Instruments and Methods in Physics Research Section A: Accelerators, Spectrometers, Detectors and Associated Equipment*, vol. 740, pp. 60–66, 2014.

[9] A. Giribono *et al.*, "6d phase space electron beam analysis and machine sensitivity studies for eli-np gbs," *Nuclear Instruments and Methods in Physics Research Section A: Accelerators, Spectrometers, Detectors and Associated Equipment*, vol. 829, pp. 274–277, 2016.

[10] Thorlabs app note: "resolution test targets". [Online]. Available: https://www.thorlabs.com/newgrouppage9.cfm?objectgroup_id=4338

[11] L. G. Sukhikh *et al.*, "Simulation of transition radiation based beam imaging from tilted targets," *Phys. Rev. Accel. Beams*, vol. 20, p. 032802, Mar 2017. [Online]. Available: https://link.aps.org/doi/10.1103/PhysRevAccelBeams.20.032802

[12] A. Variola, "Utilisation du rayonnement optique pour l'etude des caracteristiques spatiotemporelles d'un faisceau d'electrons. Application a TTF," Ph.D. dissertation, Universite de Paris-Sud, France, 1998.

[13] G. Kube, "Imaging with optical transition radiation, transverse beam diagnostics for the xfel," *TESLA-FEL Report*, vol. 1, p. 2008, 2008.

[14] G. Kube *et al.*, "Transverse beam profile diagnostics using point spread function dominated imaging with dedicated defocusing," in *4th International Particle Accelerator Conference, IPAC 2013*, 2013, pp. 488–490.

ISBN 978-3-95450-182-3